Available online at www.sciencedirect.com
ScienceDirect
Polymer 48 (2007) 1586–1595
polymer
www.elsevier.com/locate/polymer

Synthesis and viscoelastic behavior of water-soluble polymers modified with strong hydrophobic side chains

K. Podhajecka [a], K. Prochazka [a], D. Hourdet [b,*]

[a] Department of Physical and Macromolecular Chemistry, Faculty of Science, Charles University, Prague Hlavova 2030, 12843 Prague 2, Czech Republic
[b] Physico-Chimie des Polymères et des Milieux Dispersés, UMR 7615, UPMC-CNRS-ESPCI, 10 rue Vauquelin, 75005 Paris, France

Received 20 November 2006; received in revised form 26 December 2006; accepted 9 January 2007
Available online 13 January 2007

Abstract

A new series of associating polymers were prepared by grafting highly hydrophobic side chains: poly(*n*-butyl acrylate), *PNBA*; poly(*n*-butyl methacrylate), *PNBMA*; and poly(*N*-(*tert*-butyl)acrylamide), *PTBA* of different sizes onto a poly(sodium acrylate), *PAANa*, backbone. Due to the strong hydrophobic character of the stickers, the dynamics of the associations is very slow as compared to more conventional water-soluble polymers modified with short alkyl chains and the physical associations mainly behave as chemical ones in the experimental conditions. As a consequence, all the copolymers readily self-assemble in aqueous solution forming clusters in very dilute conditions and then gels at higher concentrations. From dynamic measurements, it was shown that the copolymer solutions follow the same scaling relation $\eta^* \sim c^a$, where a is a frequency dependent exponent. In these conditions, all the copolymer solutions exhibit a sol–gel transition which obeys the main rules of the percolation theory. For each copolymer, the critical gel concentration c_g depends strongly on the hydrophobic character of the stickers and a single master curve can be drawn by plotting the complex viscosity vs. the reduced concentration, c/c_g. Although the temperature dependence of the viscoelastic properties is very weak, due to the slow dynamics of the associations, it was clearly evidenced that the alkyl acrylamide derivative (PAANa-*g*-PTBA) exhibits a slight thermothickening behavior which contrasts with the thermothinning behavior of alkyl(meth)acrylate derivatives (PAANa-*g*-PNBA and PAANa-*g*-PNBMA). The opposite type of behavior is explained by the presence of the amide function which is known to play an important role in the LCST (lower critical solution temperature) phase diagram of *N*-alkyl derivatives.

Keywords: Poly(acrylic acid); Associating polymers; Sol–gel transition

1. Introduction

Water-soluble polymers with hydrophobic substituents have been extensively studied from the theoretical and experimental points of view due to their important role as thickeners and viscosity modifiers in a variety of water-borne technologies including paints, inks and cosmetics. These polymers are tailored on the basis of a hydrophilic structure, ensuring the overall solubility in water, covalently bound with hydrophobic moieties. The general idea is to control the viscosity of the solutions through the formation of large intermolecular networks due to the self-association of hydrophobic moieties – stickers in the aqueous media. Among parameters that influence the behavior of physical networks belong the polymer architecture, the extent of hydrophobic modification and the binding energy of stickers. According to theoretical works in this field [1–6], the relaxation time of the network is closely related to the lifetime of the sticker in the hydrophobic domain, τ_b:

$$\tau_b = \tau_0 \exp(W/kT) \quad (1)$$

Here τ_0 is a microscopic time related to the characteristic frequency of the thermal vibration ($\tau_0 \sim 1$ ns), k is the Boltzmann constant, T is the absolute temperature and W is

* Corresponding author. Tel.: +33 (0)1 40 79 46 43; fax: +33 (0)1 40 79 46 40.
E-mail addresses: podhajec@imc.cas.cz (K. Podhajecka), prochaz@vivien.natur.cuni.cz (K. Prochazka), dominique.hourdet@espci.fr (D. Hourdet).

0032-3861/$ - see front matter © 2007 Elsevier Ltd. All rights reserved.
doi:10.1016/j.polymer.2007.01.013

the potential barrier depending both on the binding energy and on the additional activation barrier.

Polymers modified by stickers with moderate values of the binding energy [7–13], typically short alkyl chains (C6–C20) [7,12,13] have attracted the largest scientific interest. They form reversible networks with short relaxation times: for instance, the solutions of the so-called HEUR telechelic polymers – poly(ethylene oxide), PEO, end capped by dodecyl and octadecyl stickers – are characterized by relaxation times 0.001 and 0.8 s, respectively [7]. Much less attention was devoted to the associating polymers with longer or more hydrophobic stickers and higher binding energies. Cathebras et al. [14] studied HEURs with perfluoroalkylated end caps. Compared to the fully hydrogenated homologue, the relaxation time of $CF_3(CF_2)(CH_2)_{11}$ end-capped PEO was three orders of magnitude longer. Telechelic poly(sodium acrylate) with long polystyrene end caps (23 monomeric units) studied by Tsitsilianis et al. [15,16] was also characterized by high terminal relaxation times in the order of hundreds of seconds.

The aim of the present study is to investigate the role of non-conventional stickers, with high binding energy in water, on the rheological properties of associating polymers. For this purpose we prepared a series of grafted copolymers (Fig. 1) based on the same poly(sodium acrylate) backbone modified by different hydrophobic oligomeric side chains: poly(*n*-butyl acrylate), *PNBA*; poly(*n*-butyl methacrylate), *PNBMA*; and poly(*N*-(*tert*-butyl)acrylamide), *PTBA*.

The low affinities of these materials to water are documented by the values of solubility parameters. For example, the solubility parameters estimated by Hoy method [17] $\delta_2 = 18.8$, 19.4 and 21.8 $MPa^{1/2}$ for PNBMA, PNBA and PTBA, respectively, are very different from the solubility parameter $\delta_1 = 47.9$ $MPa^{1/2}$ for water. According to these values, the dissolution of a PNBMA chain containing 30 monomeric units would require energy about 3000 kJ/mol which is about two orders of magnitude higher than that of conventional stickers, e.g., dodecyl ($\sim$40 kJ/mol).

Another important aspect taken into account in the selection of grafts was their response to temperature changes in relation to their mixing behavior in water. Associating copolymers designed with stickers displaying a lower critical solution temperature in water (LCST) are well known for instance for their thermoassociating properties [18–22]. Upon temperature increase above LCST, the stickers lose their initial affinity to water and their local aggregation gives rise to the formation of a physical network. From this point of view, both PNBA and PNBMA differ significantly from PTBA. The latter belongs to the family of *N*-substituted acrylamide derivatives that cover a wide scale of solubility behavior in water [23]. It starts with poly(*N*-methyl acrylamide) and poly(*N*,*N*-dimethyl acrylamide) which are fully soluble in water at all temperatures and goes through poly(*N*-ethyl acrylamide) and poly(*N*-isopropyl acrylamide) that display the LCST behavior around 32 °C and extends to more hydrophobic derivatives such as PTBA. In the last section of this paper, it will be shown that PTBA, although insoluble in water at all temperatures, gives rise to interesting thermothickening properties when used as a sticker in associating polymers.

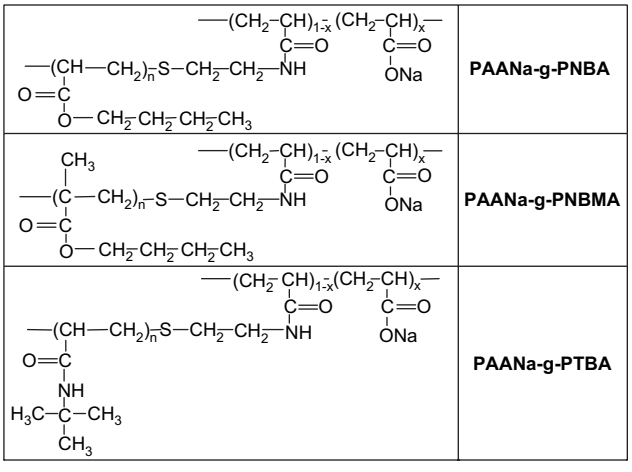

Fig. 1. Structure of grafted copolymers.

2. Experimental

2.1. Materials

Monomers *n*-butyl acrylate (NBA), *n*-butyl methacrylate (NBMA) and *N*-(*tert*-butyl)acrylamide (TBA) were obtained from Aldrich and used as received without further purification. Poly(acrylic acid), PAA ($M_w = 270$ kg/mol, $M_n = 90$ kg/mol), was purchased from Aldrich under sodium salt form, PAANa. It was neutralized under acidic form (PAAH) by HCl and purified by ultrafiltration (membrane cut-off 30 kD) before concentration and freeze-drying. Analytical grade reagents: 2-aminoethanethiol hydrochloride (Fluka); azobis(isobutyronitrile), AIBN (Fluka); 1,3-dicyclohexylcarbodiimide, DCCI (Aldrich); and organic solvents from SDS: *N*,*N*-dimethylformamide, DMF; 1-methyl-2-pyrrolidone, NMP; methanol; ethanol; 1-butanol; and acetone were used as received.

2.2. Synthesis of grafts

About 10 g of monomer was dissolved in 100 mL of DMF and heated under nitrogen at 75 °C for 40 min. Aminoethanethiol hydrochloride was then added at a given molar ratio: $R_0 = (telogen)/(monomer)$. AIBN of 0.1 g, previously dissolved in 5 mL of DMF and shortly bubbled by nitrogen, was introduced into the reaction vessel and the reaction mixture was kept at 75 °C under nitrogen for 5 h. After cooling, the reaction mixture was precipitated in a sodium hydroxide aqueous solution in order to remove HCl from $NH_3^+Cl^-$ end groups. *PNBA–NH_2* and *PNBMA–NH_2* formed a paste-like phase in water which was removed and dried under vacuum pump. *PTBA–NH_2* powder was filtered, dried overnight under vacuum and then dissolved in a small amount of THF. The polymer was finally recovered by precipitation in a large excess of hexane (500 mL), filtration and drying under vacuum pump.

2.3. Grafting

PAAH of 5 g was dissolved in 150 mL of NMP at 60 °C overnight. Telomer of x g and DCCI of $0.3x$ g (molar ratio [DCCI]/[amine] ~ 8), previously dissolved in 30 and 20 mL of NMP, respectively, were added. The reaction mixture was let under stirring for 8 h at 60 °C. After cooling, the copolymer was neutralized by addition of a small amount of a concentrated aqueous solution of NaOH. Under ionization, the copolymer phase separates and forms a polymer rich phase which was recovered and pressed in order to remove the maximum of NMP.

2.4. Purification

The copolymers PAANa-*g*-PNBA, PAANa-*g*-PNBMA and PAANa-*g*-PTBA were dissolved in a minimum volume of water and precipitated in a large volume (~1 L or more) of organic non-solvent: butanol/ethanol (3:1), acetone and ethanol, respectively. After filtration, the precipitate was washed several times in the corresponding non-solvent before drying under vacuum. Finally, all the copolymers were purified by dialysis for one week against pure water (membrane cut-off 6–8 kD), to eliminate the excess of NaOH, and freeze dried.

^{1}H NMR was performed on a Bruker Avance 400 MHz spectrometer. Telomers were characterized in $CDCl_3$. The composition of grafted copolymers was determined under acidic form: PAANa-*g*-PNBA and PAANa-*g*-PNBMA in deuterated DMF and PAANa-*g*-PTBA in deuterated ethanol.

2.5. Size exclusion chromatography

It was carried out on Waters 150 CV+ chromatographic system using dual detection: a differential viscometer coupled with a differential refractometer (Waters R410). Molecular characterization of telomers was performed in THF at 40 °C using four Ultrastyragel columns (10^3, 10^4, 10^5 and 10^6 Å) calibrated with PS standards. PAA was characterized by SEC in aqueous solution ($LiNO_3$ 0.5 mol/L) at 20 °C using four Shodex OH-pak columns calibrated with PEO standards.

2.6. Rheometry

The measurements were performed on a strain-controlled rheometer, Rheometrics RFS2, equipped with a cone/plane geometry (diameter = 50 mm, angle 2°, truncation = 45 μm). The experiments were performed in the linear viscoelastic regime which was first determined for each sample by a dynamic strain sweep. All the samples under sodium salt form (full ionization) were dissolved in distilled water and gently stirred for several days until homogeneous solutions were obtained. Then the samples were left to equilibrate for at least two days.

3. Results and discussion

3.1. Synthesis and characterization

The synthesis of grafted copolymers was carried out in two steps. First, amino-terminated hydrophobic oligomers were prepared by radical telomerization. In the second step the amino end groups of telomers were coupled with carboxylic groups of the poly(acrylic acid) backbone. The telomerization, carried out with the aminoethanethiol as transfer agent (telogen), introduces a $NH_2-CH_2-CH_2-S-$ group at the chain ends giving rise to functionalized oligomers displayed in Fig. 2.

The telomers were characterized by SEC and ^{1}H NMR (see Fig. 3 and Table 1). The number average degree of polymerization, as estimated by NMR, is calculated by comparing the methylene signals of the functional group to the signals of the monomeric units. By comparison to SEC data, the degree of polymerization of oligomers obtained by NMR is generally higher even if we take into account the accuracy range of

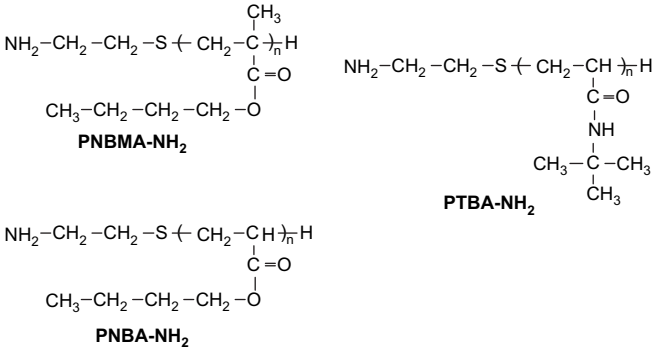

Fig. 2. Amino functionalized telomers: poly(*n*-butyl methacrylate), PNBMA–NH_2, poly(*n*-butyl acrylate), PNBA–NH_2 and poly(*N*-(*tert*-butyl)acrylamide), PTBA–NH_2.

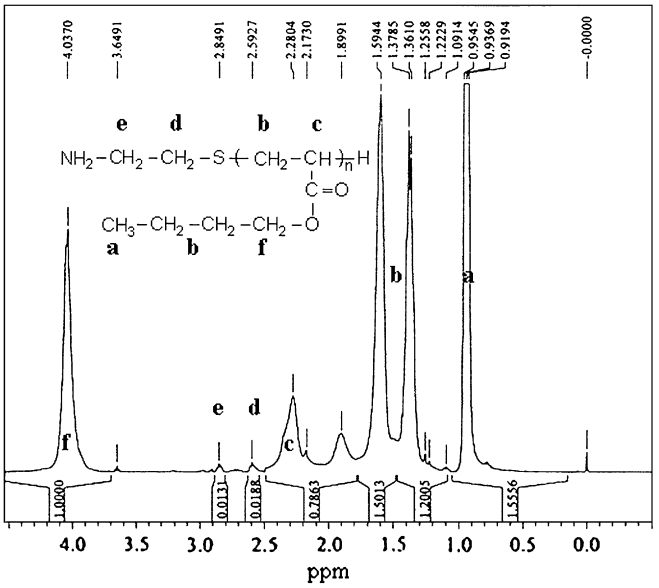

Fig. 3. ^{1}H NMR spectrum of PNBA6300 ($R_0 = 0.08$) in $CDCl_3$ (400 MHz).

Table 1
Molecular characteristics of telomers

Telomer	Feed ratio		^{1}H NMR	SEC			
	R_0	$1/R_0$	DP_n	DP_n	M_n	M_w	I_p
PNBMA6100	0.04	25	76 ± 20	42	6100	17 400	2.9
PNBMA4500	0.08	12.5	33 ± 7	31	4500	12 500	2.8
PNBA6800	0.05	20	76 ± 12	53	6800	18 800	2.8
PNBA6300	0.08	12.5	65 ± 13	49	6300	18 900	3.0
PTBA4900	0.1	10	–	38	4900	17 700	3.6
PTBA6800	0.1	10	74 ± 24	53	6800	16 800	2.5

the data. This difference can be explained considering that all the chains have not been initiated by the telogen and that consequently some of them are not effectively tagged by the $NH_2-CH_2-CH_2-S-$ terminal group. In other words, the degree of polymerization determined by NMR is overestimated and this discrepancy indicates that a fraction of chains has not been initiated directly by the telogen. This assumption has been verified by "matrix assisted laser desorption ionization-time of flight" mass spectrometry (MALDI-TOF). This method is not suitable to characterize the molecular weights of polydisperse samples but it provides additional information concerning the end groups and the functionalization of oligomers. From the molar mass distribution of PNBMA ($R_0 = 0.08$) given in Fig. 4, it can be seen that the peaks are evenly spaced with $\Delta m = 142$ g/mol which corresponds to the molar mass of *n*-butyl methacrylate unit.

The main peaks correspond to oligomeric chains initiated by $NH_2-CH_2-CH_2-S$. However, a homologous series of weaker intensity can be observed with a shift of −8, as referred to the previous one.

These oligomers correspond to polymer chains which were directly initiated from radicals coming from AIBN decomposition. Similar results were also obtained for other oligomers. This result can be related to a low transfer activity of the telogen and seems realistic considering the high values of the molar masses which were obtained. Normally, if the chain transfer constant C_T is close to unity, the polymerization degree of the telomers remains constant during the conversion and equals to the value of $1/R_0$, where R_0 is the initial ratio between telogen and monomer in the reaction mixture [24]. In our case the number average degree of polymerization determined by SEC is 2–5 times higher than the values of $1/R_0$. The comparison is not obvious as we have probably lost the low molecular weight species during the precipitation of telomers. Nevertheless, the only way to consider the existence of telomer chains with DP_n higher than $1/R_0$ is to assume that the chain transfer constant is lower than 1 [24,25]. In the literature, the chain transfer constants are reported to vary considerably with the nature of the monomer, the functionality of the telogen and with the solvent [25–31]. However, for a series of telogens ($HS-CH_2-CH_2-R$), the reactivity increases for $R = -NH_2 < -COOCH_3 < COOH < -CONHNH_2$ [28]. The low telogen activity of aminoethanethiol hydrochloride was also observed during telomerization of *N*-(2-hydroxypropyl)methacrylamide and methyl methacrylate in DMF [28,31].

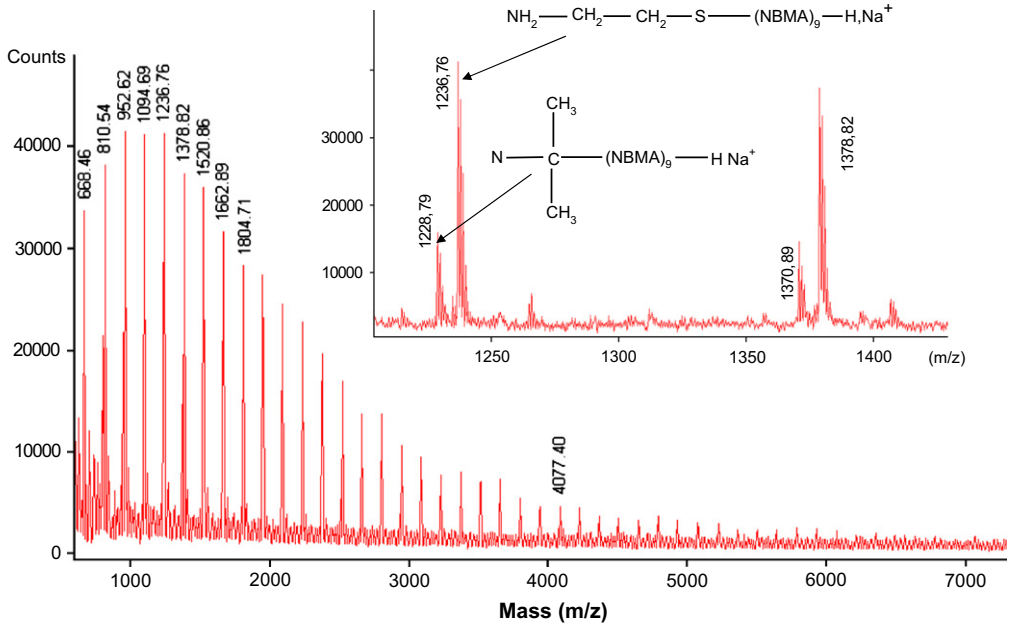

Fig. 4. Molar mass distribution of PNBMA4500 obtained by MALDI-TOF.

From Table 1, it can be seen that for PNBMA and PNBA series, the molar mass increases with increasing R_0 as expected from the telomerization mechanism. However, the degree of polymerization is not proportional to $1/R_0$ indicating that the fractionation of telomers that certainly occurs during their purification strongly influences the molecular weight distribution. This is clearly the case of the two PTBA samples which display distinct molar masses ($M_n = 4900$ and 6800 g/mol) although they have been prepared in similar conditions ($R_0 = 0.1$).

In the second step of the synthesis, the telomers were grafted onto the PAA backbone by coupling amino end groups to carboxylic acids. This condensation is activated by dicyclohexylcarbodiimide (DCCI) which is a well-known coupling agent [19,32,33]. According to the NMR analysis performed on grafted copolymers, the yield of the grafting reaction ranges between 60 and 100%. This supports the previous discussion concerning the functionality of oligomers obtained by radical telomerization where a majority of polymer chains, but not all, were effectively initiated by the telogen.

The list of grafted copolymers synthesized on the basis of the same PAA backbone is given in Table 2 The copolymers are denoted according to their composition, molar mass of grafts as determined by SEC and weight fraction of grafts in the copolymer where PAA is in the form of sodium salt. For example, PAANa-*g*-PNBA6800(4) stands for a copolymer containing 4 wt% of grafts of poly(*n*-butyl methacrylate) of molar mass 6800 g/mol.

3.2. Associating behavior

In Fig. 5, the dynamic complex viscosity of different grafted copolymers measured at 1 rad s^{-1} is compared with the steady shear viscosity of the backbone precursor (PAANa) measured under similar conditions at $\dot{\gamma} = 1\ s^{-1}$. For small concentrations up to about 4 wt% PAANa, the solutions obey to the scaling law $\eta \sim c^{0.5}$, while at higher concentrations the slope of the curve starts to follow higher power law. According to the Fuoss relation, the viscosity of polyelectrolyte solutions in dilute and unentangled semidilute regimes follows $\eta \sim c^{1/2}$ at low ionic strength. In the entangled semidilute regime of salt-free

Table 2
Primary structure and scaling behavior of PAA grafted with highly hydrophobic stickers

	w_{graft}	N_g	x_T	c_g (wt%)	n	tan δ	n^*
PAANa-*g*-PNBMA6100(16)	0.16	2.8	16	0.09	0.8	1.6	0.6
PAANa-*g*-PNBA6300(16)	0.16	2.8	5.7	0.2	0.6	1.3	0.6
PAANa-*g*-PNBMA4500(9)	0.09	1.9	2.9	0.35	0.7	1.8	0.7
PAANa-*g*-PNBMA6100(7)	0.07	1.1	–	0.5	0.7	1.8	0.7
PAANa-*g*-PTBA6800(23)	0.23	4.0	1.3	0.9	0.6	1.6	0.6
PAANa-*g*-PTBA4900(18)	0.18	4.0	1	1.5	0.6	1.7	0.7
PAANa-*g*-PNBA6800(4)	0.04	0.5	–	>5.3			

w_{graft}, weight fraction of grafts in the copolymer; N_g, average number of grafts per backbone; x_T, shift factor as obtained from Fig. 6; c_g, critical gel concentration; n – slope of log G' and log G'' vs. log ω at c_g – loss tangent (tan δ (G''/G')) at c_g; and n^*, relaxation exponent calculated from the loss tangent: $n^* = (2/\pi)\arctan(G''/G')$.

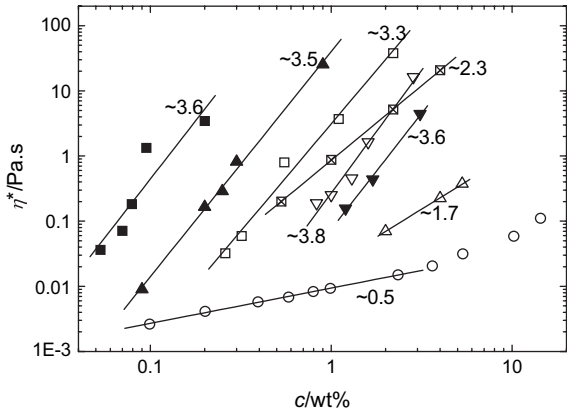

Fig. 5. Double logarithmic plot of complex viscosity, η^* as a function of polymer concentration, c, for different copolymers ($\omega = 1$ rad s^{-1}) {■ – PAANa-*g*-PNBMA6100(16), ▲ – PAANa-*g*-PNBA6300(16), □ – PAANa-*g*-PNBMA4500(9), ⊠ – PAANa-*g*-PNBMA6100(7), ▽ – PAANa-*g*-PTBA6800(23), ▼ – PAANa-*g*-PTBA4900(18), △ – PAANa-*g*-PNBA6800(4)} and ○ – PAANa backbone ($\dot{\gamma} = 1\ s^{-1}$). The viscosities obey the scaling laws $\eta \sim c^a$ or $\eta^* \sim c^a$; corresponding fits and scaling exponents, a, are given.

polyelectrolyte solutions, Dobrynin et al. predicted that $\eta \sim c^{3/2}$ [34]. In our case the transition between unentangled and entangled regimes occurs above 4 wt% and it can be concluded that all grafted copolymers were studied in the unentangled semidilute regime. In the same figure, we can also verify that the critical entanglement concentration occurs at about $\eta \approx 50\ \eta_s$ (where η_s is the viscosity of the solvent: 10^{-3} Pa s for water) which is a general criterion that holds for both neutral and polyelectrolyte chains [34].

From Fig. 5, it can be immediately realized that the complex viscosities of grafted copolymers are several orders of magnitude higher than the viscosity of their PAANa precursor: a strong associative behavior is thus clearly evidenced. Using the analogy with other associating water-soluble copolymers, it can be concluded that the association is due to hydrophobic domains formed by side chains that interconnect the soluble backbones forming a 3D polymeric network. It should be noted here that unlike PAANa solutions, the dynamic complex viscosities of grafted copolymers are strongly frequency dependent and no Newtonian plateau has been observed in the frequency window $\omega = 0.1–100$ rad s^{-1}, as it will be shown later. However, in order to compare the different copolymers and to illustrate their associative behavior, the complex viscosity at 1 rad s^{-1} was used for the determination of scaling relations.

An interesting observation is that at 1 rad s^{-1}, the scaling exponents vary around 3.6 for all studied copolymers with only two exceptions: PAANa-*g*-PNBA6800(4) and PAANa-*g*-PNBMA6100(7) that display very low scaling exponents 1.7 and 2.3, respectively. This particular behavior can be explained by the very small average number of grafts per chain in these two copolymers that are 0.5 and 1.1, respectively. These macromolecular samples contain only a minor fraction of backbones having at least two grafts, which are able to participate in the formation of physical cross-links. Remaining

polymer chains, which are non-grafted or that possess only one graft per chain, are not elastically active and tend to lower the viscoelastic properties of the network. Solutions of poorly grafted copolymers display intermediate scaling law behavior between grafted and non-grafted systems.

If we consider only the series of grafted copolymers which contain enough side chains and exhibit similar scaling relation, we can draw a master curve of the rheological behavior by shifting the different curves along the concentration axis and setting the sample PAANa-*g*-PTBA4900(18) as reference (Fig. 6). In that case, the shift factor x_T, reported in Table 2, becomes a quantitative indicator of the association process and association strength. From the collection of results given in Table 2 and Figs. 5 and 6 some general trends can be retrieved that reveal the relation between the structure of copolymers and their ability to increase the viscosity of the solutions. Three decisive parameters can be taken into account: the chemical nature of the grafts, their molar mass and the mass fraction of grafts in the copolymer. The effect of the molar mass of grafts can be depicted using the comparison between PAANa-*g*-PTBA6800(23) and PAANa-*g*-PTBA4900(18). As a matter of fact, these two copolymers have the same average number of grafts per backbone (4) and they differ only in the graft length. As expected, a more pronounced associating behavior is found in the case of PAANa-*g*-PTBA6800(23) that possess grafts of a higher degree of polymerization.

When comparing PAANa-*g*-PNBMA6100(16) and PAANa-*g*-PNBMA6100(7), that are grafted to different extents with the same side chains, it can be concluded that the less grafted PAANa-*g*-PNBMA6100(7) is a weaker thickener. As previously described, this effect can be attributed to the very small average number of grafts per backbone turning a fraction of chains elastically inactive.

The influence of the chemical nature of grafts can be evaluated when PAANa-*g*-PNBMA6100(16), PAANa-*g*-PNBA6300(16) and PAANa-*g*-PTBA6800(23) are compared. PAA-*g*-PNBMA6100(16) clearly shows the most pronounced associating behavior of all the copolymers involved in the present study. Its viscosity is more than one order of magnitude higher than that of PAANa-*g*-PNBA6300(16) which has the same weight fraction of grafts with practically the same molar mass. PAANa-*g*-PTBA6800(23) which is more densely grafted with hydrophobic side chains of slightly higher molar mass is however the worst thickener of the three. In terms of concentration, the same level of viscosity can be reached by using 10 times less of PAANa-*g*-PNBMA6100(16) than PAANa-*g*-PTBA6800(23). These trends correlate with the affinity between grafts and water molecules. The solubility parameters estimated from the Hoy method [17] for PTBA, PNBA and PNBMA are $\delta_2 = 21.8$, 19.4 and 18.8 $MPa^{1/2}$, respectively. In this series, the affinity to water ($\delta_1 = 47.9$ $MPa^{1/2}$) decreases while the capacity of polymers to enhance the viscosity of the solution increases. In Fig. 5 only the complex viscosity measured at one particular frequency ($\omega = 1$ rad s^{-1}) was reported. Taking into account the whole set of data, obtained in the frequency range $\omega = 0.1-100$ rad s^{-1}, we have plotted in Fig. 7 the frequency dependence of the scaling exponent a ($\eta \sim c^a$). In the comparison, only the copolymers containing sufficient numbers of grafts per backbone were taken into account. It was shown previously that the copolymer samples follow a unique scaling relation with an exponent $a \cong 3.6$ for $\omega = 1$ rad s^{-1}. From Fig. 7 we can see that the scaling exponent strongly depends on the frequency but remains almost independent of the sample structure in the whole frequency range.

The strong dependence of a in the whole range of frequency under investigation can be correlated to the very high binding energy between hydrophobic side chains which do not relax in the timescale of the rheological experiments. The highest coefficients ($a = 4.5-5.5$) obtained at the lowest frequency ($\omega = 0.1$ rad s^{-1}) are similar to those reported with associating systems above the percolation threshold [5,18].

3.3. Sol–gel transition

A typical set of rheological patterns obtained upon dilution is shown in Fig. 8 taking PAANa-*g*-PNBA6300(16) as a representative example. At relatively high concentrations a strong gel behavior is observed (Fig. 8, curve a).

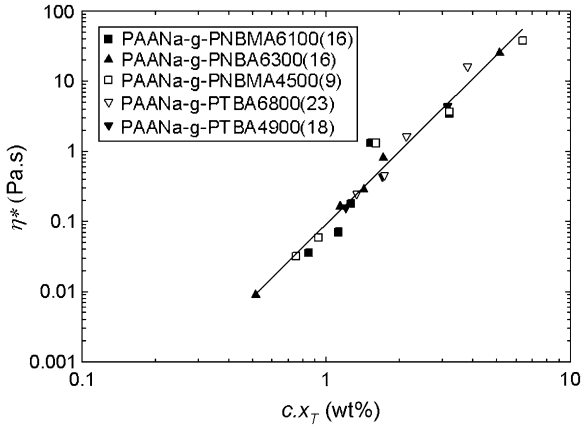

Fig. 6. Master curve of the complex viscosity vs. relative concentration. The values of the shift factor x_T, applied to the different samples, are reported in Table 2.

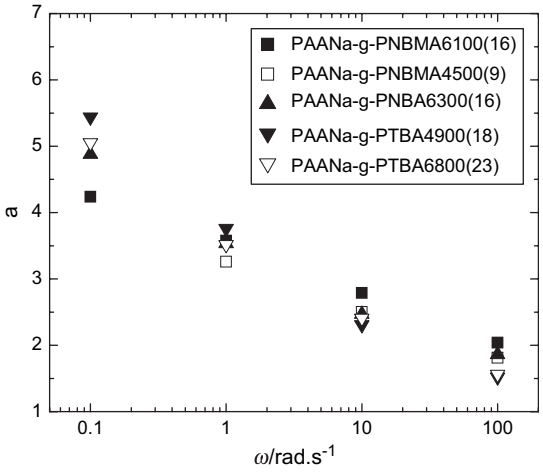

Fig. 7. Frequency dependence of the exponent a obtained from the scaling law: $\eta^* \sim c^a$ for the series of copolymer samples.

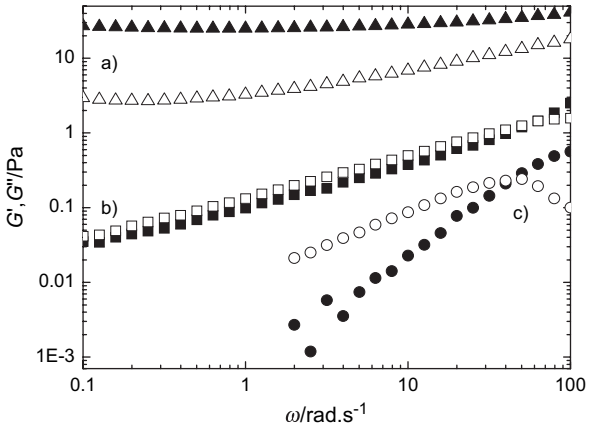

Fig. 8. Typical rheological patterns – storage (full symbols) and loss (open symbols) moduli vs. frequency – obtained at different concentrations of PAANa-*g*-PNBA6300(16) copolymer: (a) 0.91, (b) 0.2 and (c) 0.09 wt%.

The storage modulus is weakly dependent on frequency and is superior to the loss modulus in the whole frequency range explored. The longest relaxation time is too long to be determined within the observation timescale $t = 10-0.01$ s corresponding to frequencies $\omega = 0.1-100$ rad s^{-1}. This behavior is due to the strong hydrophobic interactions between grafts that strongly slow down the dynamics of the physical gel. Within the observation window, the graft does not leave its aggregate and the gel structure is not allowed to relax (the chains remain attached to the same domains). As the concentration is decreasing, both the storage and loss moduli decrease and become more frequency dependent. At about $c = 0.2$ wt%, the storage and loss moduli become parallel (Fig. 8, curve b) and the loss tangent, G''/G', is invariant of frequency in a broad frequency range. This critical feature corresponds to the mechanical behavior of systems at the gel point as described by Winter and Chambon [35,36]. In the present case, the gelation concentration threshold $c_g \cong 0.2$ wt% can be determined for PAANa-*g*-PNBA6300(16). At this concentration, the relaxation exponent (n) is equal to $= 0.55-0.6$, as it can be calculated either from

$$n = (2/\pi)\arctan(G''/G') = 0.58 \tag{2}$$

or from the slopes of the frequency dependence of the moduli [37,38]:

$$G' \sim G'' \sim \omega^n \tag{3}$$

Below the critical concentration there are not enough polymers to fill the space and a collection of independent clusters is observed. Even though no macroscopic phase separation occurs, the rheological characteristics progressively change. At concentrations well below the gel point a Maxwellian behavior is observed as shown in Fig. 8 (curve c) with a crossover of G' and G'' at $\omega_c = 50$ rad s^{-1} corresponding to a characteristic time $\tau_c = 1/\omega_c = 0.02$ s. Considering the strong binding interaction of PNBA grafts, this short characteristic time cannot be correlated with the lifetime of a graft in the hydrophobic domain but it must correspond to the dynamics of the cluster itself issued from the fractionation of the gel.

It should be emphasized that the concentration dependence of rheological patterns displayed by PAANa-*g*-PNBA6300(16) is common to all copolymers involved in the present study, but the different regimes: strong gel, gel point, solution of clusters occur for different copolymers at different concentrations. The values of critical gel concentration, c_g, can thus conveniently serve for comparison of the individual copolymers. In Table 2, where the copolymers are listed in the decreasing order of their thickening ability (results obtained from Fig. 5), we can verify that the best thickener has the lowest critical gel concentration and that the sol–gel transition is shifted to higher concentrations when the associating behavior decreases. We can also notice that the critical gel concentration (c_g) is inversely proportional to the shift factor (x_T) and that $x_T c_g$ remains constant for all copolymers and equals 1–1.5. This result brings to the fore that all copolymer solutions follow the same rules during the association process and that c_g is really the key parameter for the description of the associating behavior. As a matter of fact, the viscoelastic properties of the copolymer solutions can be normalized in the whole concentration range (see Fig. 6) by using the reduced concentration cx_T, or c/c_g, which is totally equivalent.

At the sol–gel transition, all the copolymer solutions show relaxation exponents n varying between 0.6 and 0.7 (see Table 2). These data are in a good agreement with the relaxation exponents currently reported for both chemical and physical gels in the literature [39–42]. Increasing values of n, from 0.5 to 0.7, were also reported by Chambon and Winter [36] for chemical networks when changing the stoichiometry by increasing the cross-linker deficiency. All these results clearly underline the fact that associating polymers tailored with highly hydrophobic stickers follow a unique behavior during gel formation which has a lot of similarities with the percolation theory.

This theory predicts a universal scaling behavior in the sense that all properties can be expressed in powers of the distance from the gelation point ($p - p_g$) where p is the progress of the gelation and p_g its value at the gelation point. In physical gelation, p depends on the cross-linking mechanism; it may be temperature, curing time, concentration, etc. In the present case, the key parameter is the concentration and we will use the relative distance from the gelation point $\varepsilon = |(c - c_g)/c_g|$ which is more useful to draw a general comparison between the different associating copolymers. For a viscoelastic system characterized by a zero shear viscosity η_0 and a shear plateau modulus G_0, the exponents used to describe the singularities near the gel point are n (Eq. (2)), s and t given by:

$$\eta_0 \sim \varepsilon^{-s} \quad \text{for } c < c_g \tag{4}$$

$$G_0 \sim \varepsilon^{t} \quad \text{for } c > c_g \tag{5}$$

These parameters are related to each other by the following relation:

$$n = t/(s+t) \tag{6}$$

In order to apply the percolation theory to the copolymer solutions, we have plotted in Fig. 9 the variation of the

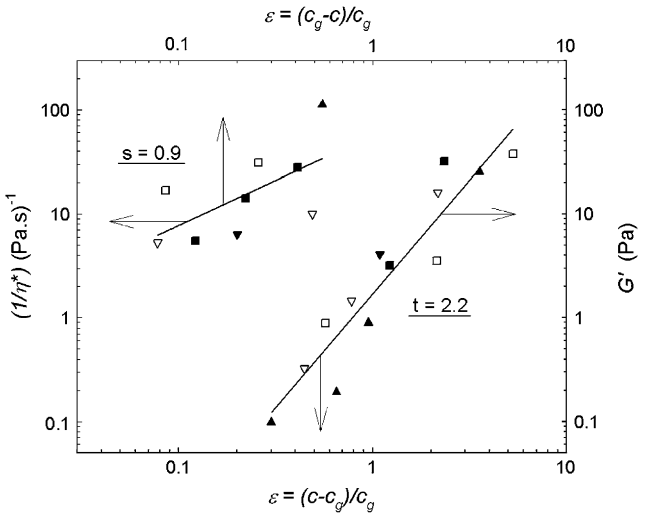

Fig. 9. Variation of complex viscosity (η^*) and elastic modulus (G') with the relative distance from the gel point ε. Experiments were performed at $\omega = 1$ rad s^{-1}.

complex viscosity (η^*) and elastic modulus (G') as a function of the relative distance from the gel point $\varepsilon = |(c - c_g)/c_g|$. It can be readily seen that the percolation theory describes fairly well the associating behavior and the sol–gel transition of associating copolymers developed with highly hydrophobic stickers. Despite the lack of data below the gel point, linear regressions give experimental scaling exponents $s = 0.9$ and $t = 2.2$ (and $n = 0.71$) which are in good agreement with the theoretical ones calculated in the framework of the electrical network analogy: $s = 0.75$, $t = 1.9$ and $n = 0.72$. In this model, the determination of scaling exponents lies on an analogy suggested by de Gennes between the elasticity of an incomplete network of springs, which describes the elasticity of a gel and the conductivity of a percolating conductor network in an insulating medium [43]. Nevertheless, we have to keep in mind that the main difficulties generally found close to the gelation threshold are related to the exact determination of the Newtonian viscosity (η_0) and the plateau modulus (G_0). In the present conditions used to probe the scaling relations ($\omega = 1$ rad s^{-1}), both complex viscosity (η^*) and elastic modulus (G') display some weak frequency dependence, respectively, below and above c_g. For instance, at higher frequency ($\omega = 10$ rad s^{-1}) the scaling parameters obtained are $s = 0.74$, $t = 1.8$ and $n = 0.71$ and we will only consider the qualitative agreement between the sol–gel process of our copolymer solutions and the percolation theory, rather than the pseudo-quantitative arguments.

Initially developed for chemical gelation, the percolation theory provides interesting tools to describe the formation of physical gels in conditions where the lifetime of the physical cluster (τ) is much larger than the experimental time (t) under consideration in the gel experiment, i.e. high Deborah number $De = \tau/t$. These conditions seem to be fulfilled in the case of PAA grafted with highly hydrophobic stickers.

From Figs. 6 and 9, it can be seen that the thickening properties of the associating polymers follow the main rules of the percolation theory. All the copolymers effectively undergo similar changes upon concentration increase, namely transition from a solution of microclusters through the gelation point to physical network with very long terminal relaxation time.

This typical behavior depends to a large extent on the architecture of the macromolecules as it is documented by comparison with other grafted copolymers. For instance, associating copolymers containing short alkyl side chains display very different properties for comparable extent of grafting. This is the case of poly(sodium acrylate) modified by 10 wt% of dodecyl grafts [44], which exhibit higher gel concentration threshold ($c_g = 2$ wt%). PAANa-*g*-C12 has a lot of short side chains characterized by a small binding energy as compared with PNBMA, PNBA or PTBA. One of the consequences is that the characteristics of the sol–gel transition, as described by Winter and Chambon, cannot be observed with PAA-*g*-C12 solutions as the criterion corresponding to a high Deborah number is not fulfilled [44].

Oppositely, a similar behavior to those obtained with the highly hydrophobic series have also been reported with other associating copolymers, like PAA end-capped with relatively long polystyrene, PS, chains (23 monomeric units, $M_n = 2400$ g/mol) [16]. This copolymer forms highly elastic gels at low concentrations ($c_g \cong 0.2$ wt%), characterized by parallel elastic and loss dynamic moduli (independent of frequency) and long relaxation times. The authors report $\eta^*(\omega) \sim c^{5.9}$ at 0.1 rad s^{-1} and $\eta(\gamma) \sim c^{4.2}$ at 1 s^{-1} with scaling arguments close to our average values $a = 5.0$ at 0.1 rad s^{-1} and $a = 3.6$ at 1 rad s^{-1}.

Clearly, the physical gelation mechanism, as observed with associating polymers tailored with highly hydrophobic compounds, is strongly correlated to the high binding energy between stickers. In that case, the lifetime of hydrophobic side chains in micellar junctions is substantially longer than the observation timescale. As a consequence, it appears that the dynamics of copolymer solutions remains roughly independent of the chemical substitution. It also explains why a common viscoelastic behavior has been obtained for a relatively large range of copolymer composition (2–4 grafts per backbone, graft molar mass 4500–6800 g/mol, different hydrophobic characters of grafts). On the other hand, the nature of grafts may influence the equilibrium structure that is formed during the sample preparation on timescales of several days. The strength of the hydrophobic interactions controls the concentration dependence of the cluster growth (and therefore the critical gel concentration) and subsequent gel formation.

3.4. Temperature dependence

To compare the behavior of our systems with respect to the temperature the Andrade equation was used:

$$\eta^* = B \exp(E_a/RT) \tag{7}$$

where η^* is the complex viscosity, E_a is the activation energy and B is a constant [45].

Table 3
Activation energies for water solutions of grafted PAA copolymers at different concentrations of c

System	c (wt%)	Activation energy (kJ/mol)
PAANa-*g*-PNBA6300(16)	0.7	17
	0.09	17
PAANa-*g*-PNBMA6100(16)	0.3	7
PAANa-*g*-PTBA6800(23)	1.3	−8
	2.9	−13

The activation energies obtained from the slopes of Arrhenius plots (η^* vs. $1/RT$) are listed in Table 3 for the copolymers at different concentrations.

The absolute values of E_a are comparable to activation energies of small molecules, e.g. solvents (water: 18 kJ/mol) or aqueous solutions of non-associating polymers at moderate concentrations ($c < 5\%$) [45]. They are in contrast to substantially higher values reported usually for associating polymers [7,9,14,46] where the activation energy of the viscous flow is directly related to the activation energy of the elementary process: the disengagement rate of the sticker from the junction. In the case of PNBA and PNBMA derivatives, the unexpectedly low activation energies can be correlated to the very slow dynamics of the stickers between aggregates and solution which cannot be probed within the experimental conditions ($T = 10-70$ °C, $\omega = 0.01-100$ s).

An interesting point is that, whereas the PNBA and PNBMA grafted copolymers have small but positive activation energies (both elastic and viscous moduli slightly decrease with temperature), the PAANa-*g*-PTBA solutions are characterized by a slight increase of viscosity upon heating (Fig. 10) corresponding to negative values of E_a. These opposite behaviors mainly originate from the type of carbonyl groups in the hydrophobic side chains (ester or amide) which can interact in very different ways with water molecules. PTBA for instance belongs to the family of *N*-alkyl acrylamide derivatives that display responsive solubility in aqueous media as a function of temperature. While the enthalpy of mixing of poly(*N*-alkyl acrylamide) in water is an exothermic process (with the formation of hydrogen bonds between amide groups and water molecules), the formation of a structured water shell around the hydrophobic groups is mainly exoentropic. These thermodynamic properties give rise to a LCST phase separation process which occurs at different temperatures according to the nature of the hydrophobic groups [23]. In the case of poly(*N*-isopropyl acrylamide), PNIPAM, which was studied in detail [47], the dehydration process of monomeric units and the phase separation are observed at about $T = 32$ °C. Although PTBA is not soluble in water, even at low temperatures due to the very hydrophobic *tert*-butyl group, its insolubility is enhanced by increasing the temperature as it must be the case for most LCST polymers. Like PNIPAM above its LCST, we can postulate that PTBA chains are not fully dehydrated at room temperature and that residual water molecules still interact with polar groups and self-rearrange upon heating. This can also be attributed to the high glass transition temperature of these copolymers and their aqueous mixtures which will progressively release solvent from the glassy aggregate upon heating. The associating behavior of PAANa-*g*-PTBA in water thus increases with temperature contrary to the PAA modified by poly(alkyl(meth)acrylate) side chains like PNBA and PNBMA. The same antagonistic properties were reported at high temperature, for the same reasons, for aqueous solutions of PAANa-*g*-PNIPAM and PAANa-*g*-C12 which exhibit opposite rheological properties with the temperature, namely thermothickening and thermothinning [44].

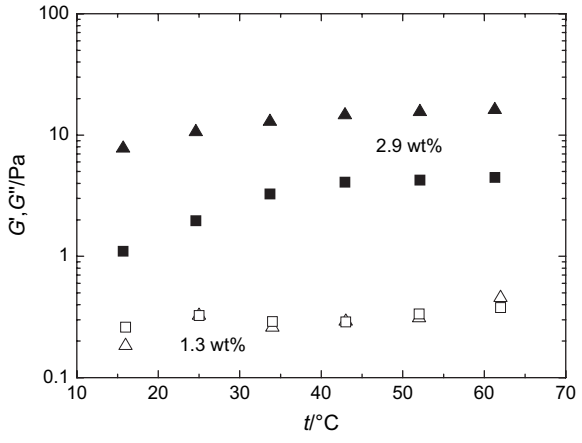

Fig. 10. Temperature dependence of storage (G', triangles) and loss (G'', rectangles) moduli (at 1 rad s^{-1}) for PAANa-*g*-PTBA6800(23) aqueous solutions at 1.3 and 2.9 wt%.

4. Conclusions

We have prepared a series of associating copolymers based on a PAA backbone grafted with different types of very hydrophobic grafts in order to probe their influence on the self-assembling properties in aqueous media. Most of copolymer solutions were characterized by a pronounced thickening behavior due to very low concentrations, which is unusual when compared with other conventional copolymers designed with the same backbone like PAANa-*g*-C12. Using dynamic experiments, we have clearly evidenced the existence of a sol–gel transition for these systems and the critical concentration (c_g) of gelation was determined for each copolymer. It was shown that for a given macromolecular backbone, c_g decreases with (1) increasing hydrophobicity of the side chains, (2) increasing molar mass and (3) increasing number of stickers. In the vicinity of the sol–gel transition, the viscoelastic properties of the solutions follow the rules of the percolation theory and this was attributed to a common mechanism of cluster growth controlled by the very slow dynamics of the associations. Above c_g, the solutions display a stiff gel behavior where the storage modulus remains always higher than the loss modulus. It was not possible to determine the terminal relaxation time as all the solutions are characterized by relaxations substantially longer than the timescale of the rheological experiments. It can be only estimated that the relaxation occurs within the order of hours. This unique

behavior can be explained by the strong hydrophobicity of the grafts together with their relatively high degree of polymerization that leads to a very high binding energy. From the rheological point of view, the behavior of studied systems resembles to that of chemically cross-linked networks. Besides the high dynamic moduli and long terminal relaxation times that exceed the timescale of the experiments, this behavior is also characterized by low apparent activation energies. For PNBMA and PNBA derivatives, the activation energy is slightly positive and reflects the influence of thermal motions of connected PAA backbones where the relaxation process of the side chain is out of scale of the experiments. An outstanding behavior is displayed by poly(*tert*-butyl acrylamide) derivatives which show slightly negative activation energy. This is caused by the ''intrinsic'' LCST behavior of this derivative characterized by some enhancement of the mutual hydrophobic interactions between grafts by disruption of the hydrogen bonds between water molecules and poly(*tert*-butyl acrylamide) upon heating. The choice of ester bonds (PNBMA and PNBA) or amide groups (PTBA) is consequently an important parameter which has to be taken into account in the design of associating water-soluble polymers.

References

[1] Tanaka F, Edwards SF. J Non-Newtonian Fluid Mech 1992;43:247.
[2] Semenov AN, Joanny J-F, Khokhlov AR. Macromolecules 1995;28: 1066–75.
[3] Leibler L, Rubinstein M, Colby RH. Macromolecules 1991;24:4701–7.
[4] Rubinstein M, Semenov AN. Macromolecules 1998;31:1386–97.
[5] Rubinstein M, Semenov AN. Macromolecules 2001;34:1058–68.
[6] Semenov AN, Rubinstein M. Macromolecules 2002;35:4821–37.
[7] Annable T, Buscall R, Ettelaie R, Whittlestone D. J Rheol 1993;37(4): 695–726.
[8] Regalado EJ, Selb J, Candau F. Macromolecules 1999;32:8580–8.
[9] Caputo MR, Selb J, Candau F. Polymer 2004;45:231–40.
[10] Tam KC, Farmer ML, Jenkins RD, Basset DR. J Polym Sci Part B Polym Phys 1998;36:2275–90.
[11] Tam KC, Ng WK, Jenkins RD. J Appl Polym Sci 2004;94:604–12.
[12] Petit-Agnely F, Iliopoulos I. J Phys Chem B 1999;103:4803–8.
[13] Petit-Agnely F, Iliopoulos I, Zana R. Langmuir 2000;16:9921.
[14] Cathebras N, Collet A, Viguier M, Berret J-F. Macromolecules 1998; 31:1305–11.
[15] Tsitsilianis C, Iliopoulos I, Ducouret G. Macromolecules 2000;33: 2936–43.
[16] Tsitsilianis C, Iliopoulos I. Macromolecules 2002;35:3662–7.
[17] Brandrup J, Immergut EH, Grulke EA. Polymer handbook. Wiley: A Wiley Interscience Publication; 1999.
[18] Bromberg L. Macromolecules 1998;31:6148–56.
[19] Hourdet D, L'Alloret F, Audebert R. Polymer 1997;38:2535.
[20] Hourdet D, L'Alloret F, Durand A, Lafuma F, Audebert R, Cotton J-P. Macromolecules 1998;31:5323–35.
[21] Durand A, Hervé M, Hourdet D. Stimuli-responsive water soluble and amphiphilic polymers. In: ACS symposium series. Washington DC: American Chemical Society; 2000. p. 181.
[22] Barbier V, Hervé M, Sudor J, Brulet A, Hourdet D, Viovy J-L. Macromolecules 2004;37:5682–91.
[23] Liu HY, Zhu XX. Polymer 1999;40:6985–90.
[24] Boutevin B, Pietrasanta Y. Telomerisation. In: Comprehensive polymer science. New York; 1989. p. 185.
[25] Loubat C, Javidan A, Boutevin B. Macromol Chem Phys 2000;201:2845.
[26] Boutevin B, Rigal G, El Asri M, Lakhlifi T. Macromol Chem 1996; 197:2273.
[27] Pichot C, Pellicier R, Grossetete P, Guillot J. Macromol Chem 1984;185:113.
[28] Lu ZR, Kopeckova P, Wu Z, Kopecek J. Bioconjugate Chem 1998;9:793.
[29] Desponds A, Freitag R. Langmuir 2003;19:6261.
[30] Costioli MD, Berdat D, Freitag R, Andre X, Muller AHE. Macromolecules 2005;38(9):3630–7.
[31] Chujo Y, Kobayashi H, Yamashita Y. J Polym Sci Part A Polym Chem 1989;27:2007–14.
[32] Chen G, Hoffman AS. Nature 1995;373:49.
[33] Wang KT, Iliopoulos I, Audebert R. Polym Bull 1988;20:577.
[34] Dobrynin AV, Colby RH, Rubinstein M. Macromolecules 1995;28:1859.
[35] Winter HH, Chambon F. J Rheol 1986;30:367.
[36] Chambon F, Winter HH. Polym Bull 1985;13:499.
[37] Stauffer D. Phys Rep 1979;54:1.
[38] de Gennes PG. Scaling concepts in polymer physics. Ithaca, NY: Cornell University Press; 1979.
[39] Cuvelier G, Launay B. Makromol Chem Macromol Symp 1990;40:23.
[40] Axelos M, Colb M. Phys Rev Lett 1990;64:1457.
[41] Yu JM, Dubois Ph, Teyssie Ph, Jerome R, Blancher S, Brouers F, et al. Macromolecules 1996;29:5384–91.
[42] Matricardi P, Dentini M, Crescenzi V. Macromolecules 1993;26:4386.
[43] de Gennes PG. J Phys Lett 1976;37:L1.
[44] Hourdet D, Gadgil J, Podhajecka K, Badiger MV, Brulet A, Wadgaonkar PP. Macromolecules 2005;38(20):8512–21.
[45] Krevelen vDW, Hoftyzer PJ. Properties of polymers. Amsterdam, Oxford, New York: Elsevier; 1976.
[46] Ng WK, Tam KC, Jenkins RD. J Rheol 2000;44(1):137–47.
[47] Cho EC, Lee J, Cho K. Macromolecules 2003;36:9929–34.